

Simultaneous Determination of Thicknesses and Refractive Indices of Ultrathin Films by Multiple Incidence Medium Ellipsometry

Jürgen Kattner and Helmuth Hoffmann*

*Institute of Applied Synthetic Chemistry, Vienna University of Technology,
Getreidemarkt 9, A-1060 Wien, Austria*

Received: March 5, 2002; In Final Form: July 24, 2002

It is shown in this paper that the thickness d_{film} and the refractive index n_{film} of a monolayer film can be determined simultaneously by single wavelength ellipsometry in different ambient media. Self-assembled alkylsiloxane monolayers were adsorbed on silicon from dilute solutions of alkyltrichlorosilane precursors ($\text{C}_n\text{H}_{2n+1}\text{SiCl}_3$, $n = 12, 18$) and the ellipsometric phase angle Δ was recorded as a function of time between the start value Δ_{sub} of the blank substrate and the final value Δ_{film} of the complete monolayer film in different solvents. From the obtained phase angle differences $\Delta_{\text{film}} - \Delta_{\text{sub}}$ of a particular monolayer film in different solvents, the unknown film parameters d_{film} and n_{film} could be calculated by numerical methods. To optimize the light incidence angle for each particular solvent, a variable angle setup was developed, which required no modifications of the standard instrument optics and utilized a standard spectrophotometric glass cell to hold the sample in contact with the ambient solvent. The two model samples of this study yielded values of $d_{\text{film}} = 26.4 \text{ \AA}$ and $n_{\text{film}} = 1.540$ for the C_{18} monolayer and $d_{\text{film}} = 18.8 \text{ \AA}$ and $n_{\text{film}} = 1.500$ for the C_{12} monolayer, showing the expected decrease in film thickness for the shorter-chain compound as well as a concomitant reduction of the film refractive index due to a less ordered, looser packed film structure.

Introduction

Ellipsometry is a well-established, straightforward technique for the determination of optical constants and thicknesses of thin adsorbate films.¹ It is based on the measurement of changes in the state of polarization of light upon reflection from the sample surface, which are expressed by two quantities called the ellipsometric angles Δ and Ψ . These measured parameters are related to the sample's reflection coefficients r_s and r_p for s- and p-polarized light by

$$\tan \Psi \exp(i\Delta) = \frac{r_p}{r_s} \quad (1)$$

For the classical three-phase system substrate/film/ambient,¹ Δ and Ψ depend on the instrumental setup (incidence angle Θ and wavelength λ of the probing radiation), on the optical properties (refractive index n , absorption index k) of substrate, film, and ambient phase, and on the film thickness d_{film}

$$\Delta = f(\Theta, n_{\text{amb}}, \lambda, d_{\text{film}}, n_{\text{film}}, k_{\text{film}}, n_{\text{sub}}, k_{\text{sub}}) \quad (2a)$$

$$\Psi = g(\Theta, n_{\text{amb}}, \lambda, d_{\text{film}}, n_{\text{film}}, k_{\text{film}}, n_{\text{sub}}, k_{\text{sub}}) \quad (2b)$$

Each measurement yields two quantities Δ and Ψ and allows, in principle, the determination of two unknown parameters from the right-hand side of eq 2, by a solution of the nonlinear equation system (2a) and (2b). Θ , λ , and n_{amb} are usually known, and the substrate constants n_{sub} and k_{sub} can be determined from a measurement of the blank substrate. If the adsorbate film is nonabsorbing ($k_{\text{film}} = 0$), a second measurement of the film-covered substrate is sufficient to obtain the two remaining unknowns: the film thickness d_{film} and the film refractive index n_{film} . This straightforward procedure is applicable as long as the changes in Δ and Ψ due to film formation exceed the

instrumental errors. In the ultrathin film regime ($d_{\text{film}} \leq 10 \text{ nm}$), however, the corresponding changes in Ψ , in particular, become extremely small and require highly precise measurements together with sophisticated calibration procedures to determine both the thickness and refractive index of an adsorbate layer.^{2–6} The alternative approach is to neglect these minute changes in Ψ but to carry out two measurements of Δ under variation of either the incidence angle Θ or the ambient refractive index n_{amb} . From a practical point of view, changing the incidence angle is much easier than changing the incidence medium and does not perturb the sample in any manner. A number of previous studies have therefore been devoted to experimental and theoretical aspects of multiple incidence angle (MIA) ellipsometry applied to a variety of different samples.^{1,7–10}

For ultrathin films, however, there is again a limitation arising from a so-called cross-correlation of n_{film} and d_{film} .^{7,8} Measurements of Δ at two angles of incidence may not deliver two independent equations (2a) for a calculation of n_{film} and d_{film} , but a set of linearly dependent equations with no unique solution. In this case, either n_{film} or d_{film} must be known to obtain the correct set of film constants and little is gained in comparison to a single fixed-angle measurement. Another possibility to obtain a set of independent equations is a variation of the incidence medium. This technique has been used previously¹¹ for the characterization of Si/SiO₂ substrates with relatively thick oxide films ($d_{\text{SiO}_2} \approx 30 \text{ nm}$), aiming at the determination of the optical constants of substrate (Si) and oxide (SiO₂) without stripping the oxide layer and being able to measure the bare substrate separately. Although the subject of that paper was quite different to the present study, the higher accuracy of the multiple incidence medium (MIM) method in comparison to the MIA technique was clearly demonstrated. From the experimental point of view, varying the ambient refractive index is a much more challenging task: First, the measurements must be carried

out under liquid ambient media to allow distinct variations of n_{amb} . Second, a set (at least a pair) of chemically inert but optically different liquids must be found, which do not perturb the film composition and structure in any way and cover a sufficiently large range of refractive indices. And third, for optimum sensitivity, the incidence angle must be adapted to the refractive index of the incidence medium, i.e., a variable angle setup with the sample contained in a liquid cell must be constructed. The majority of cell designs described for liquid media in the literature are based on a trapezoidal cell shape,¹² where the incident and reflected radiation transsect the cell windows at normal incidence and its polarization state is conserved. However, small deviations from normal incidence as well as window birefringence or dichroism may already introduce large errors in the measured angles Δ and Ψ .¹³ Moreover, a trapezoidal cell can only be used at one specific incidence angle, which would require a series of different cells for variable-angle measurements. A few other cell designs with adjustable incidence angles have been described,^{11,14} their construction and usage, however, appears to be rather complex and not suitable for the purpose of this study.

The present paper will demonstrate the feasibility of multiple incidence medium ellipsometry for the investigation of self-assembled monolayers of long-chain organosilane compounds on silicon substrates. These films represent an important and intensely studied class of adsorbate systems^{15–20} with a wide range of practical applications. They are also well suited as test samples for ellipsometric studies, because they form densely packed, oleophobic surface layers in a variety of different solvents²⁰ and usually emerge completely dry from the adsorbate solution. Thus, they represent the closest practical approach to the substrate/film/ambient model with sharp phase boundaries and a well-defined film thickness. A suitable choice of the organosilane precursor compounds allows fine-tuning of the chemical and physical properties of the resulting monolayer films, e.g., of the film thickness or the film refractive index.^{16,19–21} A novel sample cell design based on a standard commercial spectrophotometer cuvette will be described, which allows measurements in a wide range of different solvents with continuously adjustable incidence angles.

Results and Discussion

Multiple Incidence Angle (MIA) Ellipsometry versus Multiple Incidence Medium (MIM) Ellipsometry. To compare MIA and MIM ellipsometry for the characterization of ultrathin films, we have chosen as a model system a 2.6 nm thick adsorbate film with a refractive index $n_{\text{film}} = 1.54$ on a native Si/SiO₂ substrate in contact with a liquid ambient medium, representing a typical sample of this study: a long-chain hydrocarbon film chemisorbed on a silicon substrate via self-assembly from solution. To obtain a system of independent equations for the calculation of n_{film} and d_{film} from the measured phase angles Δ at different incidence angles Θ (MIA method) or different ambient refractive indices n_{amb} (MIM method), the relative partial derivative RPD defined as

$$\text{RPD} = \frac{\partial \Delta}{\partial n_{\text{film}}} / \frac{\partial \Delta}{\partial d_{\text{film}}} \quad (3)$$

must change with either Θ or n_{amb} .⁷ Figure 1 shows the calculated RPD's for our chosen model system and two typical solvents (*n*-hexane and toluene) as a function of Θ ($n_{\text{amb}} = \text{const.}$, Figure 1A) and as a function of n_{amb} ($\Theta = \text{const.}$, Figure 1B). It is clearly seen in Figure 1A that RPD is practically

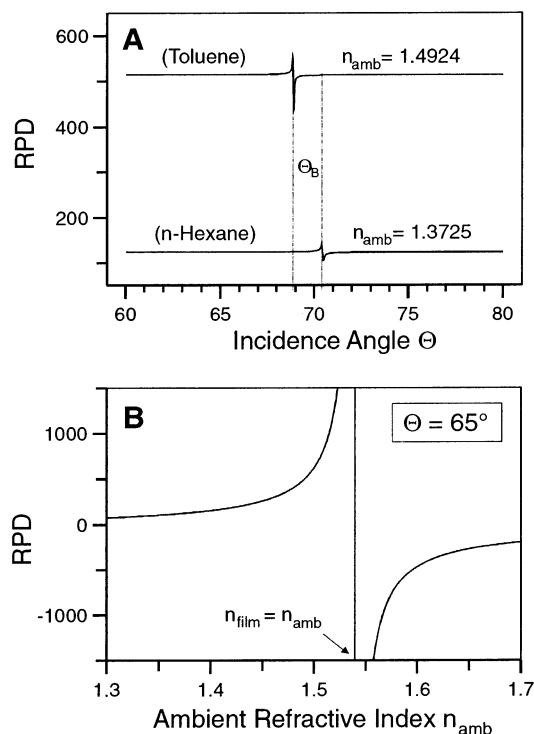


Figure 1. Simulated relative partial derivative $\text{RPD} = (\partial \Delta / \partial n_{\text{film}}) / (\partial \Delta / \partial d_{\text{film}})$ of the ellipsometric phase angle Δ for a hypothetical monolayer ($d_{\text{film}} = 2.6$ Å, $n_{\text{film}} = 1.54$) on a native Si/SiO₂ substrate (A) as a function of light incidence angle Θ for two ambient solvents and (B) as a function of the solvent refractive index n_{amb} at a constant incidence angle $\Theta = 65^\circ$. Θ_B denotes the Brewster angle of the respective ambient/substrate interface.

constant and independent of Θ in both solvents except for a narrow region of $\pm 0.5^\circ$ around the respective Brewster angles $\Theta_B = \arctan n_{\text{sub}}/n_{\text{amb}}$, where the instrumental sensitivity is too low for reliable measurements (see below). Thus, n_{film} and d_{film} are strongly correlated and cannot be determined simultaneously by variation of Θ alone. Figure 1B, on the other hand, shows that RPD varies strongly with the ambient refractive index n_{amb} (note that for $n_{\text{amb}} = n_{\text{film}} = 1.54$, RPD is not defined; similar to the region around Θ_B in Figure 1A, the instrumental sensitivity is very low for $n_{\text{amb}} \approx n_{\text{film}}$ due to the loss of optical contrast between the film and the ambient phase). Thus, variation of n_{amb} removes the cross-correlation between n_{film} and d_{film} ; i.e., measuring the phase angles Δ of the same film/substrate system in different ambient media should provide the required equations for a determination of film thickness and refractive index.

Measurements with different ambient solvents, however, require the option to adapt the incidence angle to the specific sample/solvent combination, because the phase angle change $\Delta = \Delta_{\text{film}} - \Delta_{\text{sub}}$ recorded during the growth of an adsorbate film changes strongly with Θ and has a maximum close to the principal angle Θ_P (for absorbing substrates) or the Brewster angle Θ_B (for nonabsorbing substrates) of the particular substrate/solvent system. The exact location of this sensitivity maximum depends not only on the signal magnitude Δ but also on the instrumental noise level, which is also a function of Θ and increases exponentially toward Θ_B . Figure 2 shows both quantities (the calculated signal Δ for our model sample (2.6 nm film on Si/SiO₂) and the normalized instrumental noise N measured with a blank substrate in toluene) as a function of $\Theta - \Theta_B$. The ratio of Δ/N yields the predicted signal-to-noise ratio (solid curve in the upper part of Figure 2) and has two sharp maxima about 6° off on either side of Θ_B .

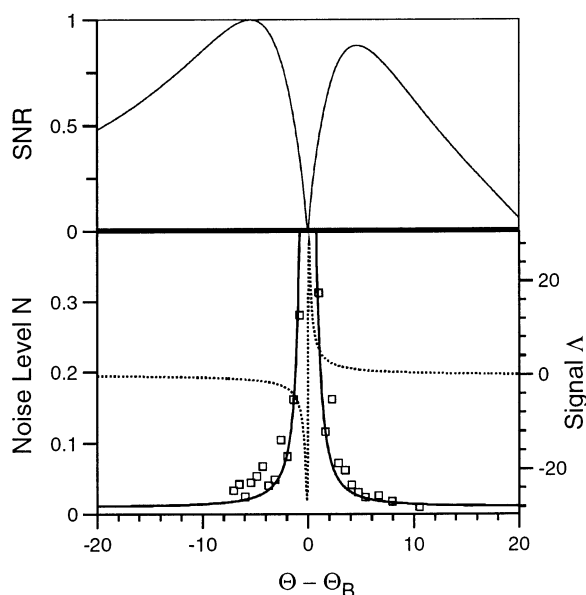


Figure 2. Simulated signal-to-noise ratio (SNR) for an ellipsometric measurement of the sample model used in Figure 1 (monolayer film on a Si/SiO₂ substrate) in a liquid ambient medium (toluene, $n_{\text{amb}} = 1.4924$) as a function of the light incidence angle Θ relative to the Brewster angle Θ_B . The dotted line in the lower diagram represents the calculated signal of the phase angle difference $\Lambda = \Delta_{\text{film}} - \Delta_{\text{sub}}$, and the solid line represents an empirical fitting curve to the instrumental noise levels shown as squares, which were determined as the standard deviation of 11 subsequent measurements of the phase angle Δ of a blank Si/SiO₂ substrate in toluene at different incidence angles. The ratio of these two curves yields the predicted SNR as a function of $\Theta - \Theta_B$ shown in the upper diagram after normalization to the range [0, 1].

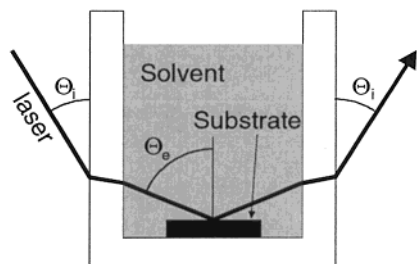


Figure 3. Liquid sample cell and light path of the probing laser for in situ ellipsometric measurements at variable incidence angles of ultrathin films formed at the substrate/solution interface. Θ_i denotes the nominal incidence angle set on the ellipsometer's angle scale and Θ_e is the effective incidence angle resulting from beam refraction at the cell/solution interface.

Construction and Performance of a Variable Angle Liquid Immersion Cell. We have chosen for this study a sample cell based on a commercial rectangular spectrophotometric cell made from optical glass. A schematic drawing of the cell and the light path of the probing laser is shown in Figure 3. The major difference between this design and previous sample cells for ellipsometric measurements with liquid ambient media (see ref 9 for an overview) is the off-normal incidence (nominal incidence angle Θ_i) of the laser beam at the cell windows. Thereby, the laser is refracted at the cell window/solution interface and hits the sample surface at an effective incidence angle Θ_e , which can be calculated for a cell with perfect rectangular geometry as

$$\Theta_e = \arccos\left(\frac{\cos \Theta_i}{n_{\text{amb}}}\right) \quad (4)$$

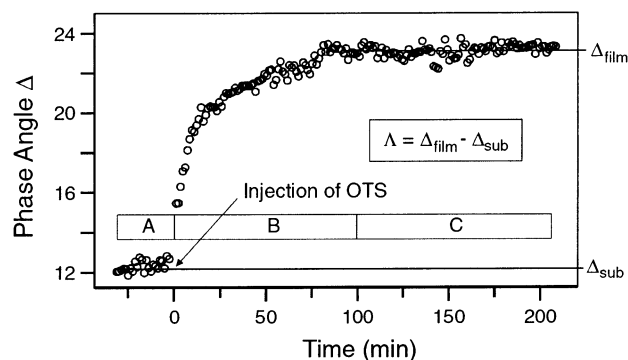


Figure 4. Ellipsometric phase angles Δ as a function of time at an incidence angle $\Theta_e = 72.19^\circ$ recording the adsorption of an octadecylsiloxane monolayer on a silicon substrate from a dilute solution of octadecyltrichlorosilane (OTS) in *n*-hexane. Each data point represents the average of five consecutive measurements within a 5 s time interval. The three time domains indicated by A, B, and C denote (A) the stabilization period for a constant start value Δ_{sub} of the blank substrate in contact with the pure solvent, (B) the sudden change of Δ after injection of the adsorbate due to film growth and (C) the saturation of Δ at the final value Δ_{film} after monolayer completion.

Θ_e depends only on the nominal incidence angle Θ_i and on the refractive index n_{amb} of the ambient medium, but not on the thickness or on the refractive index of the cell windows as long as the window faces are strictly parallel to each other. Apart from Θ_e being different from the nominal incidence angle Θ_i , the off-normal beam geometry also affects the polarization state of the probing radiation, because the Fresnel coefficients for reflection and transmission are different for s-polarized and p-polarized light,¹ contrary to a normal incidence geometry as in trapezoidal, fixed-angle liquid cells. However, if the cell window material is nonabsorbing, all Fresnel coefficients are real numbers and the ellipsometric phase angle Δ is unaltered upon transsection of the cell in the absence of window birefringence. The amplitude ratio Ψ , on the other hand, changes at the cell windows, but Ψ is too insensitive anyway, as stated before, and of little use for the characterization of ultrathin films. Another simplification and cancellation of potential errors derives from the use of the phase angle difference Λ

$$\Lambda = \Delta_{\text{film}} - \Delta_{\text{sub}} \quad (5)$$

between the phase angles of a film-covered surface Δ_{film} and of the blank substrate Δ_{sub} instead of the directly measured value Δ_{film} . If the alignment and the sample cell position in the ellipsometer are not changed between measurements of Δ_{sub} and Δ_{film} , errors due to miscalibration of the ellipsometer (inevitable for variable-angle measurements), window birefringence, or imperfect alignment of the sample cell cancel out upon subtraction according to eq 5.

In Situ Characterization of Alkylsiloxane Monolayer Films on Silicon. The formation of monolayer films of octadecylsiloxane on native silicon substrates from dilute solutions of octadecyltrichlorosilane has been extensively studied in the past^{16–20} and was therefore chosen as a test system for MIM ellipsometry with the novel cell design described above. The monolayer growth was monitored in two different solvents (toluene and *n*-hexane) at up to four different incidence angles located on either side of the respective Brewster angles Θ_B ($\Theta_B = 68.9^\circ$ for Si/toluene and $\Theta_B = 70.4^\circ$ for Si/*n*-hexane). After measuring the start value Δ_{sub} in the cell filled with 3 mL of pure solvent, 1 μL of OTS corresponding to a concentration of about 1 mmol/L was injected and the change in Δ was monitored. Figure 4 shows a representative plot of the raw

TABLE 1: Ellipsometric in Situ Measurements at Variable Incidence Angles and in Variable Ambient Solvents of the Phase Angle Differences $\Lambda = \Delta_{\text{film}} - \Delta_{\text{sub}}$ for Monolayer Films of Octadecyltrichlorosilane (OTS) and Dodecyltrichlorosilane (DTS) Formed on Native Silicon Substrates^a

adsorbent	solvent	n_{amb}	Θ_i	Θ_e	Λ	$d_{\text{film}}^{\text{(air)}}$ (Å)
OTS	toluene	1.4924	50.75	65.04	-1.73 ± 0.09	27.9
			56.00	68.12	-8.32 ± 1.33	27.3
			59.25	70.08	6.44 ± 0.68	25.5
			62.50	72.09	1.86 ± 0.18	26.1
OTS	<i>n</i> -hexane	1.3725	54.50	65.07	-3.94 ± 0.11	27.3
			59.00	68.06	-8.44 ± 0.20	27.4
			65.00	72.16	11.04 ± 0.47	26.0
			67.75	74.08	4.55 ± 0.14	27.0
DTS	<i>n</i> -hexane	1.3725	57.50	67.05	-3.38 ± 0.09	16.7
DTS	cyclohexane	1.4224	55.25	66.49	-2.24 ± 0.14	16.9

^a Θ_i and Θ_e denote the nominal and the effective light incidence angle as defined in Figure 3. n_{amb} is the refractive index of the ambient solvent, and d_{film} is the monolayer thickness measured in air as the ambient medium.

experimental data as a function of time for an OTS monolayer formed in *n*-hexane. The results of all measurements are listed in Table 1. The effective incidence angles Θ_e were calculated from the nominal angles Θ_i as described in the Experimental Section. These angles are believed to be accurate to within $\pm 0.015^\circ$ according to the instrument specifications and an error analysis of eq 7 used for the calculation of Θ_e . For the experimental error of the phase angle differences $\Lambda = \Delta_{\text{film}} - \Delta_{\text{sub}}$ listed in column 6 of Table 1, an upper limit was estimated by adding the standard deviations for the final values Δ_{film} and Δ_{sub} (Figure 4). Thus, all errors of these experimental data are believed to be upper limits. The last column in Table 1 lists the monolayer thicknesses measured after removal of the sample from the liquid cell at 68° incidence with air as the ambient medium.

An attempt to analyze the data measured in toluene by the MIA method is shown in Figure 5. A film thickness of 26 Å was used as an estimate and the phase angle difference Λ was simulated for different film refractive indices n_{film} as a function of the incidence angle Θ_e (Figure 5A). The best fit of the experimental data is obtained for $n_{\text{film}} = 1.54$. The film constants $d_{\text{film}} = 26$ Å and $n_{\text{film}} = 1.54$ obtained by this analysis are very reasonable values for an octadecylsiloxane monolayer, however, Figure 5B shows that this solution is not unique: An assumed film thickness of 52 Å yields an equally good fit for a film refractive index of 1.52. This ambiguity is a direct consequence of the cross correlation of d_{film} and n_{film} and is the essential limitation of the MIA method applied to ultrathin films: a correct solution is obtained only if one of two film parameters is known. Without any prior knowledge of either d_{film} or n_{film} , a least-squares analysis of multiple incidence angle data by the method described in the experimental part often yields wrong solutions, e.g., $d_{\text{film}} = 21.0$ Å and $n_{\text{film}} = 1.60$ for an OTS film in toluene. A very different result is obtained with data from different incidence media (MIM method). Table 2 lists different pairs of input data (Θ_e , Λ) from Table 1 measured in toluene and hexane together with the resulting calculated values for d_{film} and n_{film} . The agreement of d_{film} and n_{film} for the different sets of input data in Table 2 as well as with reported literature data for these films¹⁷ is excellent. The accuracy of the results improves only marginally, if the whole set of data listed in Table 1 is used for the calculation of d_{film} and n_{film} , resulting in $d_{\text{film}} = 26.40 \pm 0.03$ Å and $n_{\text{film}} = 1.541 \pm 0.003$. A minimum set of two independent measurements in different media is therefore

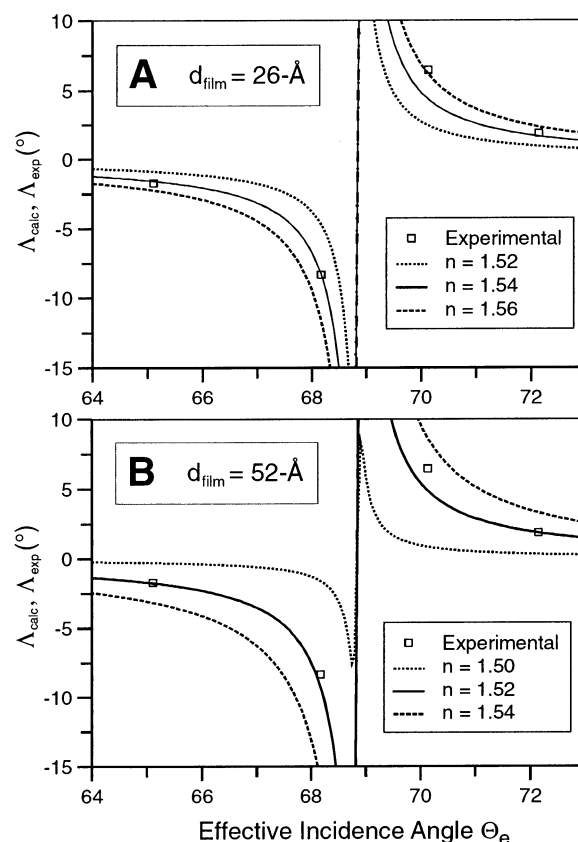


Figure 5. Experimental (square data points) and simulated phase angle differences $\Lambda = \Delta_{\text{film}} - \Delta_{\text{sub}}$ as a function of the incidence angle Θ_e for a monolayer film of OTS on silicon in contact with toluene as the ambient medium. For the simulations, a film thickness d_{film} of 26 Å (A) and 52 Å (B) and different values for the film refractive index n_{film} ranging from 1.50 to 1.56 were assumed. All other parameters for the calculations were the same as in Figure 1. The discontinuity and sign change in the Λ curves occurs at the Brewster angle $\Theta_B = 68.8^\circ$ for the toluene/silicon interface.

TABLE 2: Calculated Thicknesses d_{film} and Refractive Indices n_{film} for OTS and DTS Monolayers on Silicon from Measurements of the Phase Angle Difference $\Lambda = \Delta_{\text{film}} - \Delta_{\text{sub}}$ in Multiple Incidence Media

adsorbent	solvent	Θ_e	Λ	d_{film} (Å)	n_{film}
OTS	toluene	65.04	-1.73 ± 0.09	27.40 ± 0.06	1.540 ± 0.002
	<i>n</i> -hexane	65.07	-3.94 ± 0.11		
OTS	toluene	68.12	-8.32 ± 1.33	27.01 ± 0.06	1.541 ± 0.010
	<i>n</i> -hexane	68.06	-8.44 ± 0.20		
OTS	toluene	72.09	1.86 ± 0.18	27.84 ± 0.08	1.537 ± 0.004
	<i>n</i> -hexane	72.16	11.04 ± 0.47		
DTS	<i>n</i> -hexane	67.05	-3.38 ± 0.09	18.80 ± 0.40	1.500 ± 0.008
	cyclohexane	66.49	-2.24 ± 0.14		

sufficient for an accurate determination of the film thickness and refractive index.

As a second example, a monolayer film of dodecyltrichlorosilane (DTS) was investigated. According to previous results,^{16,18,20,21} the shorter hydrocarbon chains of this compound result in a reduced monolayer thickness compared to OTS, but also in a smaller refractive index due to the onset of structural disorder. Because the refractive index of toluene is too close to the expected film refractive index, the adsorption was carried out from 1 mmol/L solutions of DTS in *n*-hexane and cyclohexane and was monitored at an effective incidence angle of about 67° . The experimental data of these experiments as well as the calculated film thickness and refractive index are included in Tables 1 and 2. The results for d_{film} and n_{film} are in good agreement with literature data^{16,20} and with the expected trends

in comparison to OTS monolayers. An interesting difference is noticeable for DTS monolayers between the monolayer thickness of about 16.8 Å measured in air (Table 1) and the calculated thickness of 18.8 Å under in situ conditions (Table 2). Such a difference was not observed for the longer chain compound OTS and might indicate, that the more disordered and looser packed film structure of DTS tends to bind additional material (either solvent or adsorbent molecules) as long as the sample is still in contact with the adsorbate solution but loses these weakly bound molecules upon rinsing and drying of the sample prior to the ex situ characterization.

Summary and Conclusions

Thicknesses and refractive indices of nonabsorbing monolayer films can be determined simultaneously with single wavelength ellipsometry by a variation of the liquid ambient phase. Measurements of the phase angle difference $\Delta_{\text{film}} - \Delta_{\text{sub}}$ between film/substrate and blank substrate immersed in two liquids with different refractive indices yield two independent equations for the phase angles as a function of the optical constants of the sample, from which the unknown parameters d_{film} and n_{film} can be calculated. Sensitivity optimization for these measurements with multiple incidence media requires a variation of the light incidence angle, for which a novel sample optical system based on a standard spectrophotometric sample cell was developed. This instrumental setup provides a straightforward access to ellipsometric investigations of solid-liquid interfaces, which have been hampered in the past by elaborate custom-made sample cells susceptible to severe systematic errors. We are currently extending these investigations to kinetic studies of self-assembled monolayer growth processes in different solvents. Apart from the dramatic influence of the solvent on the film growth rates, another highly interesting subject of these ongoing studies is the submonolayer region of these films. The possibility to measure film thickness and refractive index of submonolayers independently might answer important outstanding questions about the nucleation and growth mechanisms of these films.

Experimental Section

Materials. The following compounds and solvents were commercially available and were used as received: *n*-octadecyltrichlorosilane (OTS, Aldrich, 95%), *n*-dodecyltrichlorosilane (DTS, ABCR, 95%), toluene (Aldrich, 99.8+% HPLC grade, $n = 1.4924$), *n*-hexane (Aldrich, 95+% HPLC grade, $n = 1.3725$), cyclohexane (Aldrich, 99.9+% HPLC grade, $n = 1.4234$), acetone (Aldrich, 99.9+% HPLC grade), ethanol (Austria Hefe AG, 99.8%). The refractive indices of the solvents were interpolated from literature data²² to the experimental conditions of this study ($\lambda = 632.8\text{-nm}$, $T = 22.5\text{ }^{\circ}\text{C}$) using a three-term Cauchy dispersion formula,²³ where a , b , and n_{∞} are solvent constants and T is the temperature

$$n = n_{\infty} + \frac{a}{\lambda^2} + \frac{b}{\lambda^4} + \frac{\partial n}{\partial T} \Delta T \quad (6)$$

Silicon wafers (100 oriented, p-doped, single-sided polished, 7–21 $\Omega\text{ cm}$ resistivity, 0.5 mm thickness) were cut into rectangular pieces of 15 \times 15 mm² and sonicated in toluene. After rinsing with toluene, acetone, and ethanol, they were dried in a stream of pure nitrogen. Subsequent treatment (2 \times 10 min) in an UV/ozone cleaning chamber (Boekel Industries, UVClean) yielded a hydrophilic, contamination free surface. The thickness

of the native oxide layer was measured ellipsometrically after this cleaning procedure using literature values for the optical constants of silicon ($n = 3.865$, $k = 0.020$) and silicon dioxide ($n = 1.465$, $k = 0$) and lay always between 11 and 13 Å.

Ellipsometer. Ellipsometric measurements were carried out using a PLASMOS SD2000 rotating analyzer ellipsometer (RAE, vertical setup) with a wavelength of 632.8 nm (HeNe laser). Both laser and analyzer arm could be aligned independently between 40° and 90° with a precision of 0.015°. The vertical position of the sample stage as well as its tilt angle could be adjusted manually and controlled with an alignment microscope. The ellipsometer was equipped with a custom-made, computer-controllable laser shutter to avoid prolonged irradiation and induced heating of the adsorbate solution. The data acquisition software was modified such that measurements could be scheduled over an arbitrary period of time.

Sample Cell Alignment. A commercial rectangular spectrophotometric cell (Hellma 402.000-OG, path length $D = 20\text{ mm}$, outer dimensions $H \times W \times D = 40 \times 23.6 \times 25\text{ mm}$) made from optical glass (DESAG B70 Superwhite, $n_D = 1.5230$) was cut to a height of 20 mm to fit into the UV/ozone cleaning chamber and the ellipsometer stage. The cell could be closed with a Teflon lid in combination with a rectangular Viton seal ($d = 1\text{ mm}$) and could be filled or emptied without exposure to the atmosphere through a hole in the cover with a flexible Teflon tubing connected to a syringe. Before each measurement, the cell was cleaned with a detergent solution, rinsed thoroughly with deionized water, acetone, and ethanol and dried with nitrogen. The Teflon cover, the Viton seal, and the gold brackets used to lock the sample in position were sonicated in toluene, rinsed with acetone, and ethanol and also dried in a stream of nitrogen. Immediately before use, the cell was exposed for 2 \times 10-min to a UV/ozone atmosphere (cleaning chamber UVClean, Boekel Industries) to remove organic contaminants, that could eventually disturb the adsorption process.

A typical measurements protocol started with mounting the substrate firmly at the cell bottom using two gold brackets. The sample cell was then mounted on the ellipsometer sample stage, and the laser arm of the instrument was moved to 90° incidence. The laser aperture was covered with a microscope glass slide coated with a thin, semitransparent silver film, which served as a monitor for the cell alignment by visualization of the laser spots transmitted from the laser source and reflected from the cell's entrance window surface. The cell was preliminarily aligned by rotation on the sample stage until the entrance window (facing the laser arm) was oriented normal to the laser beam. Using the alignment microscope, the sample stage tilt was now adjusted until the sample surface was oriented normal to the main vertical axis of the instrument. For an ideal cell geometry, the sample should be precisely aligned after this procedure and the cell windows should be exactly normal to the laser beam set for 90° incidence, as shown in Figure 6A; i.e., the transmitted and reflected spot at the semitransparent slide in front of the aperture should coincide. If this is not the case due to imperfections in the cell or sample geometry (wedge-shaped sample or cell bottom, angle between cell windows and cell bottom $\neq 90^{\circ}$), an iterative fine adjustment consisting of (1) rotation of the cell, (2) adjustment of the incidence angle, and (3) alignment of the sample stage tilt must be performed until the two laser spots coincide and the sample surface is perpendicular to the instrument axis (Figure 6B). The final laser incidence angle after this alignment equals the tilt angle θ_L between the entrance window and the sample surface and requires a correction of the previously defined effective

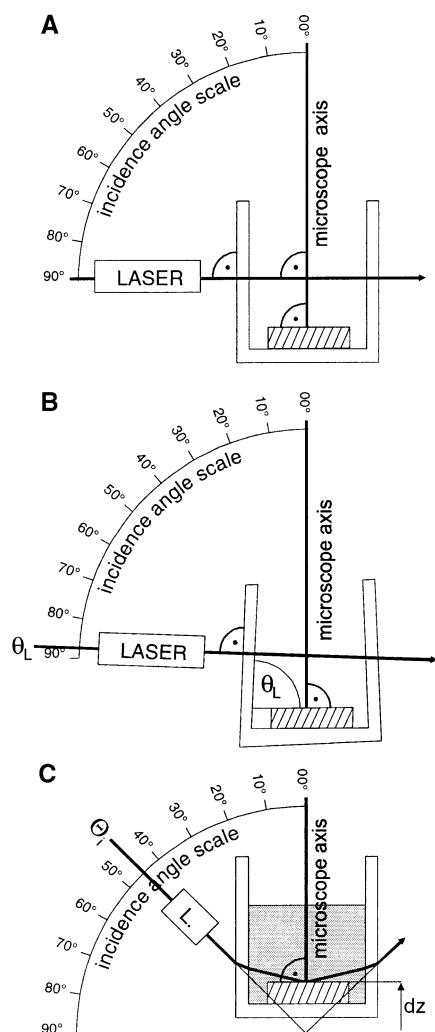


Figure 6. Alignment of the liquid cell in the ellipsometer. (A) Alignment for a perfect cell and substrate geometry with parallel surfaces and rectangular cell windows. (B) Alignment for a nonperfect cell/substrate system with tilted cell windows and/or wedge-shaped substrate or cell bottom. θ_L is the tilt angle between the entrance window and the substrate surface, which must be determined to calculate the effective light incidence angle Θ_e by eq 7. (C) Final alignment after setting the desired incidence angle Θ_i and adjusting the cell height by dz after filling the cell with solvent.

incidence angle Θ_e (eq 4) according to

$$\Theta_e = \theta_L + \arcsin\left(\frac{\sin(\Theta_i - \theta_L)}{n_{\text{amb}}}\right) \quad (7)$$

θ_L depends both on the (invariable) cell geometry and on the (variable) sample position within the cell (e.g., due to variable substrate surface tilts, wedge-effects of the sample, etc.). We have repeatedly measured θ_L in the course of this study with different substrates and have always obtained a reproducible value of $90.3 \pm 0.03^\circ$. θ_L was therefore assumed to be constant, and the above-described alignment procedure before each experiment could be simplified to a horizontal adjustment of the sample surface via the microscope optics and a vertical rotation of the sample cell until the transmitted and reflected laser spots were aligned in a vertical plane. The incidence angle of the ellipsometer was then set to the nominal incidence angle Θ_i corresponding to the desired effective angle Θ_e according to eq 7 and the cell was filled with solvent. Due to refraction at the cell window/solvent interface, a final adjustment dz of the

sample stage height was necessary, as shown in Figure 6C, until the laser beam passing through the solvent-filled cell hit the laser detector. Neither the effective incidence angle nor the cell alignment was affected by this final height adjustment.

In Situ Ellipsometric Measurements. The substrate/solvent probe was allowed to stabilize until the measured phase angles Δ assumed a constant value Δ_{sub} . Subsequently, the solvent was replaced by the adsorbate solution by either injecting a calculated amount of pure adsorbate compound into the cell or by replacing the solvent with a prefabricated adsorbate solution, whereby great care had to be taken not to change the position of sample and cell. The change of Δ due to film formation was monitored in situ until a complete monolayer had formed and Δ assumed a constant, final value Δ_{film} .

Model Calculations. Ellipsometric phase angles Δ and phase angle differences $\Lambda = \Delta_{\text{film}} - \Delta_{\text{sub}}$ were calculated according to eq 1 with assumed or experimentally determined optical constants using a computer-programmed matrix formalism for the calculation of the sample's reflection coefficients.²⁴ Film thicknesses and refractive indices were determined from experimental values Λ_{exp} by a numerical least-squares method.⁷ An error function G was defined as

$$G = \sum_{j=1}^J (\Lambda_{\text{exp},j} - \Lambda_{\text{calc},j})^2 \quad (8)$$

with j as the number of measurements of Λ_{exp} either at different incidence angles and/or in different ambient media. Initial guesses for the unknown sample parameters were used to evaluate Λ_{calc} and d_{film} and/or n_{film} were varied systematically until the minimum of G was found. A gradient search method²⁵ was used for this iteration process, which could be easily programmed for a computer.

Acknowledgment. This work was supported by the *Fonds zur Förderung der Wissenschaftlichen Forschung* (Project P 12769) and the *Jubiläumsfonds der Österreichischen Nationalbank* (Projekt 7815).

References and Notes

- (1) Azzam, R.; Bashara, N. *Ellipsometry and Polarized Light*; Elsevier: Amsterdam, 1987.
- (2) McCrackin, F.; Passaglia, E.; Stromberg, R.; Steinberg, H. J. *Res. Natl. Bur. Stand.* **1963**, A67, 363.
- (3) Easwarakhanthan, T.; Ravelet, S.; Renard, P. *Appl. Surf. Sci.* **1995**, 90, 251.
- (4) Ducharme, D.; Tessier, A.; Russev, S. C. *Langmuir* **2001**, 17, 7529.
- (5) Tiberg, F.; Jönsson, B.; Tang, J.; Lindman, B. *Langmuir* **1994**, 10, 2294.
- (6) Tiberg, F.; Jönsson, B.; Lindman, B. *Langmuir* **1994**, 10, 3714.
- (7) Ibrahim, M. M.; Bashara, N. M. *J. Opt. Soc. Am.* **1971**, 61, 1622.
- (8) Bu-Abbud, G. H.; Bashara, N. M. *Appl. Opt.* **1981**, 20, 3020.
- (9) Smit, M. K.; Verhoof, J. W. *Thin Solid Films* **1990**, 189, 193.
- (10) Rhykerd, C. L.; Cushman, J. H.; Low, P. F. *Langmuir* **1991**, 7, 2219.
- (11) Landgren, M.; Jönsson, B. *J. Phys. Chem.* **1993**, 97, 1656.
- (12) Kattner, J.; Hoffmann, H. In *Encyclopedia of Surface and Colloid Science*; Hubbard, A., Ed.; Marcel Dekker: New York, 2002.
- (13) So, S. S.; Knausenberger, W. H.; Vedham, K. *J. Opt. Soc. Am.* **1971**, 61, 124.
- (14) Ayupov, B. M.; Sysoeva, N. P. *Cryst. Res. Technol.* **1981**, 16, 503.
- (15) Ulman, A. *An Introduction to Ultrathin Films*; Academic Press: San Diego, 1991.
- (16) Wasserman, S. R.; Tao, Y.-T.; Whitesides, G. M. *Langmuir* **1989**, 5, 1074.
- (17) Parikh, A. N.; Allara, D. L.; Azouz, I. B.; Rondolez, F. *J. Phys. Chem.* **1994**, 98, 7577.
- (18) Brzoska, J. B.; Azouz, I. B.; Rondolez, F. *Langmuir* **1994**, 10, 4367.
- (19) Hoffmann, H.; Mayer, U.; Krischanitz, A. *Langmuir* **1995**, 11, 1304.

- (20) Brunner, H.; Vallant, T.; Mayer, U.; Hoffmann, H. *J. Colloid Interface Sci.* **1999**, 212, 545.
- (21) Tillman, N.; Ulman, A.; Schildkraut, J. S.; Penner, T. L. *J. Am. Chem. Soc.* **1988**, 110, 6136.
- (22) Lechner, M. D., Ed. *Optical Constants, Subvolume b, Refractive Indices of Organic Liquids*; Springer: New York, 1996.
- (23) Yakovlev, V. A.; Irene, E. A. *J. Electrochem. Soc.* **1992**, 139, 1450.
- (24) Kattner, J.; Hoffmann, H. In *Handbook of Vibrational Spectroscopy*; Chalmers, J. M., Griffiths, P. R., Eds.; Wiley: Chichester, U.K., 2002; Vol. 2.
- (25) Bevington, P. R. *Data Reduction and Error Analysis for the Physical Science*; McGraw-Hill: New York, 1992.